Supporting information

Porous Si@C Ball-in-Ball Hollow Spheres for Lithium-ion Capacitor with improved energy and power density

Bo Li,[a] Shixiong Li,[a] Ying Jin,[b] Jiantao Zai[a], Ming Chen,[a] Ali Nazakat,[a] Peng Zhan,[b] Yong Huang,[a] and Xuefeng Qian*[a]*

[a] Shanghai Electrochemical Energy Devices Research Center, School of Chemistry and Chemical Engineering and State Key Laboratory of Metal Matrix Composites, Shanghai Jiao Tong University，Shanghai 200240, China

[b] ZhongTian Emerging Materials Co. LTD, Nantong, 226000, China

Email: xfqian@sjtu.edu.cn, zaijiantao@sjtu.edu.cn

Experimental

All Chemical reagents were purchased from Shanghai Chemical Co. Ltd., and they were directly used without further purification.

Materials Preparations

$MHSiO_2$: The preparation of $MHSiO_2$ was following a procedure reported in the literature. Typically, cetyltrimethylammonium bromide (CTAB, 0.3 g) was dissolved in ethanol aqueous solution (60 mL C_2H_5OH/100 mL H_2O) containing concentrated ammonia aqueous solution (2 mL, 25 wt%). Then, tetraethoxysilane (TEOS, 2 mL) was rapidly added to the mixture under vigorous stirring. After stirring at 35 ºC for 24 h, the white precipitation was collected by centrifugation and washed with ethanol. Then, the product was dispersed in water and kept at 90 ºC for 2 h. The product collected by centrifugation was dispersed into an ethanol solution (240 mL) containing concentrated HCl (480 μL, 37%) and stirred at 60 ºC for 3 h, generating the template-free $MHSiO_2$.

$MHSiO_2@Al_2O_3$: $MHSiO_2@Al_2O_3$ nanospheres were prepared by a facile synthetic protocol in a buffer solution. In a typical synthesis, 0.63 g of ammonium formate was dispersed in 200 ml deionized water, and then formic acid was added till the pH value to 4.4. Then 0.1 g of $MHSiO_2$ and 0.3 g aluminum sulfate were added and dispersed by ultrasound treatment for 30 min. The solution was kept at 70 ºC for 2 h under vigorously stirring. The resulted core-shell NPs were collected by centrifugation, washed with water and ethanol, and dried at 80 ºC for 4 h.

$MHSiO_2@Al_2O_3@C$: Carbon coating of $MHSiO_2@Al_2O_3$ was carried out by thermal decomposition of acetylene gas at 800 ºC for 10min in a quartz furnace. The mixture of acetylene and high-purity argon (argon: acetylene = 9: 1 by volume) was introduced at a flow rate of 150 sccm.

$SiO_2@C$ ball-in-ball hollow spheres: The obtained $MHSiO_2@Al_2O_3@C$ was then immersed in a 1 M HCl solution for 6 h to remove Al_2O_3. Finally, the resulted powders were collected by filtration and washed with water for several times and vacuum-dried at 70 ºC for 6 h.

Porous Si@C ball-in-ball hollow spheres: Magnesium powder (0.3 g) was mixed with $MHSiO_2$@void@C (0.3 g) by grinding. The mixture was then heated in a tube furnace at 650 ºC for 5 h under an argon atmosphere containing 5 vol% H_2. The ramp rate was kept at 1 ºC min^{-1}. The obtained powder was then immersed in a 2 M HCl solution for 6 h to remove MgO and. Finally, the resulted powders were collected by filtration and washed with water for several times and vacuum-dried at 70 ºC for 4 h.

MHSi@SiC@C: The preparation process of Si@SiC@C is similar to the method of Si@void@C, except for the addition of void space between SiO_2 and carbon.

RAC: The RHs were firstly leached with a 10% HCl solution to remove the metal ions impurities. The leached RHs were heated to 700 ºC, and then maintained at 700 ºC for 2 h in a tube furnace under the protection of nitrogen to obtain carbonized RHs (CRHs). CRHs were mixed with KOH in a 1:5 mass ratio. The mixture was then transferred to ceramic boats and heated to 700 ºC at a ramp rate of 2 ºC min^{-1}, and then maintained at 700 ºC for 1 h in a tube furnace under nitrogen. The resultant activation products were filtered and washed with water until the filtrate became neutral. Finally, the RACs were dried at 90 ºC for 10h.

Characterization

X-ray diffraction (XRD) patterns were recorded on a D/max 2550VL/PC X-ray diffractometer (Rigaku, Japan) equipped with Cu Kα radiation (λ = 1.5418 Å, 40 kV, 30 mA). Raman spectra were acquired using an inVia-reflex micro-Raman spectrometer (Renishaw, UK) with a 532 nm wavelength incident laser. X-ray photoelectron spectroscopy (XPS) was performed on an AXIS Ultra DLD spectrometer (Kratos, Japan) with Al Kα radiation (hv = 1486.6 eV). Thermogravimetric analysis (TGA) was performed on an SDT Q600 thermoanalyzer (DSC-TGA, TA, USA) in air. The specific surface area and pore size distribution of materials were measured using a NOVA2200e analyzer (Quantachrome, USA). The morphology of samples was observed using a NOVA NanoSEM 230 field-emission scanning electron microscope

(FESEM, FEI, USA). The microstructure of samples was characterized using a JEM-2100F transmission electron microscope (TEM, JEOL, Japan) operating at 200 kV.

Electrochemical measurements

The electrochemical experiments were performed using CR2016 coin cells, which were assembled in a glove box filled with ultra-high purity argon. For half-cell testing, Si/C and RAC electrodes were used as working electrodes and Li metal as the reference electrode. The Si/C electrodes were prepared by casting a slurry consisting of 70 wt% of active material, 15 wt% poly(acrylic acid) (PAA) binder, and 15 wt% of Super-P carbon black on Cu foil. The RAC electrodes were prepared by mixing 80 wt% of active material, 10 wt% Cellulose Sodium (CMC) binder, and 10 wt% of Super-P carbon black on Al foil. The typical mass loading of the active materials in cathode and anode are 2 mg and 1 mg, respectively. 1 M $LiPF_6$ in a mixture of ethylene carbonate, dimethyl carbonate (EC/DEC, 1:1 by vol%) and 10 wt% fluoroethylene carbonate (FEC) was used as the electrolyte. The Si/C||RAC LICs were also assembly in coin cells with Si/C anode (pre-cycled for 3 cycles at 0.4 A g^{-1}) and RAC cathode in the same electrolyte, and the optimized mass ratio of anode and cathode was 1:7. The galvanostatic charge and discharge experiment were performed on a battery tester LAND-CT2001A at room temperature. The voltage range of Si/C electrode was 0.01-1.5 V, and the cell is conducted at a low current density of 0.4 A g^{-1} in the first cycle to activate the anode materials. The RAC electrodes and the Si/C||RAC LICs were measured at the same voltage range of 2.0-4.0 V. Cyclicvoltammetry (CV) was conducted on an electrochemical workstation. Electrochemical impedance spectroscopy (EIS)

measurements were performed on a ZAHNER Zennium electrochemical workstation. The energy density (E) and power density (P) were calculated form the galvanostatic charge/discharge curve by the equation

$$E = \int_{t2}^{t1} IV\, dt$$

(I)

Where E (W h kg^{-1}) is energy density, I is the constant current density (A g^{-1}), V is the voltage, and ti, t2 is the start time and end time in the discharge process, respectively.

$$P = \frac{E}{\Delta t}$$

(II)

Where P (W g^{-1}) is power density, Δt is discharge time (s). The mass includes both anode and cathode active materials.

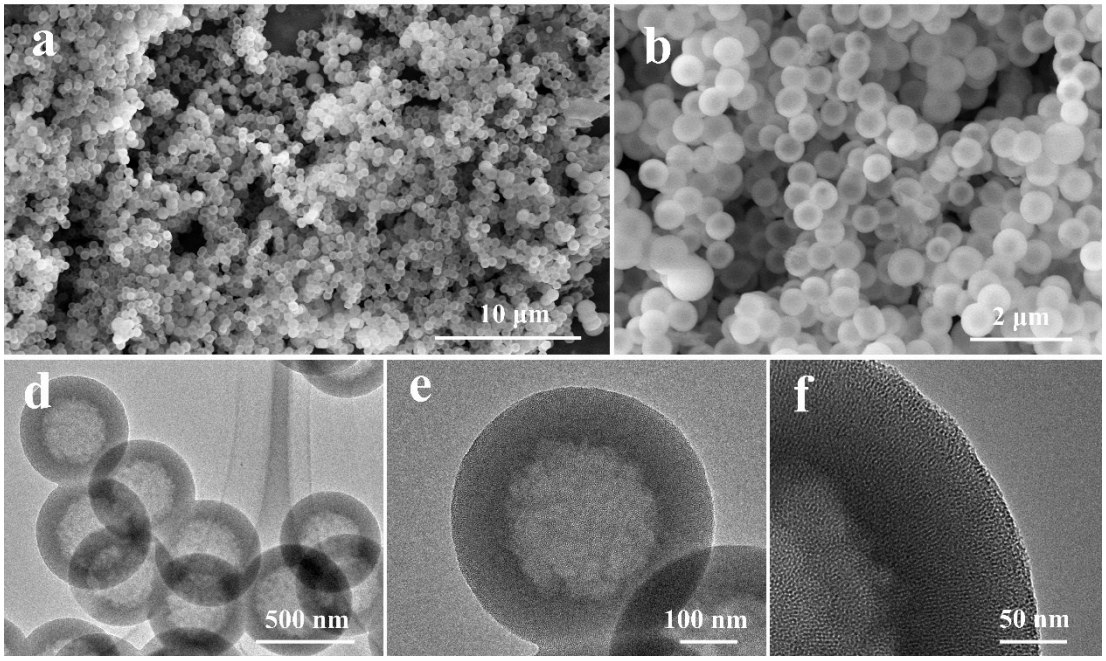

Figure S1. SEM images of (a), (b) TEM images of (d), (e) and (f) SiO_2

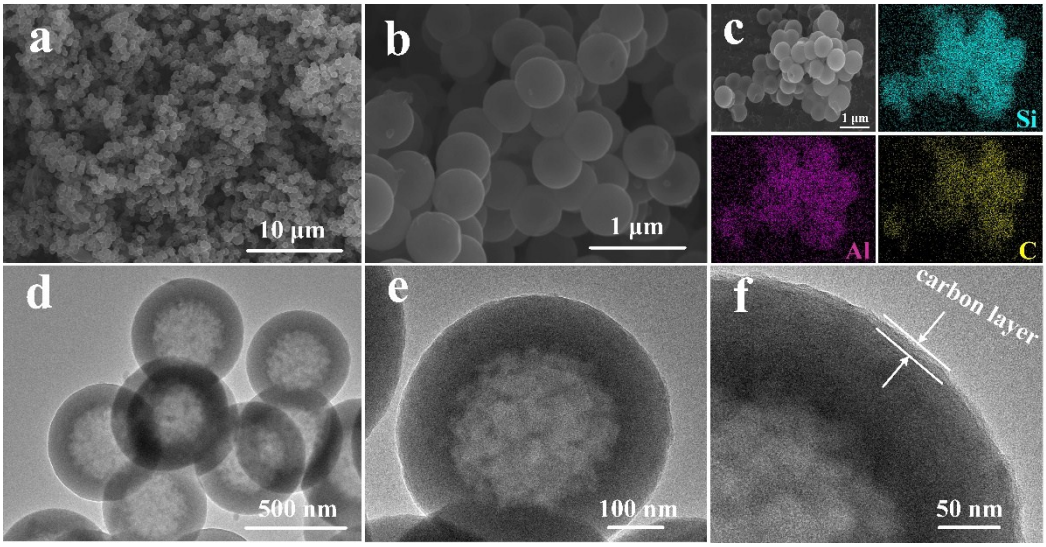

Figure S2. SEM images of $SiO_2@Al_2O_3@C$ (a) and (b). (c) SEM image of $SiO_2@Al_2O_3@C$ and corresponding EDX elemental mapping images of Si (blue), Al (purple) and C (yellow). TEM images of $SiO_2@Al_2O_3@C$ (d), (e) and (f) Magnified TEM images of $SiO_2@Al_2O_3@C$.

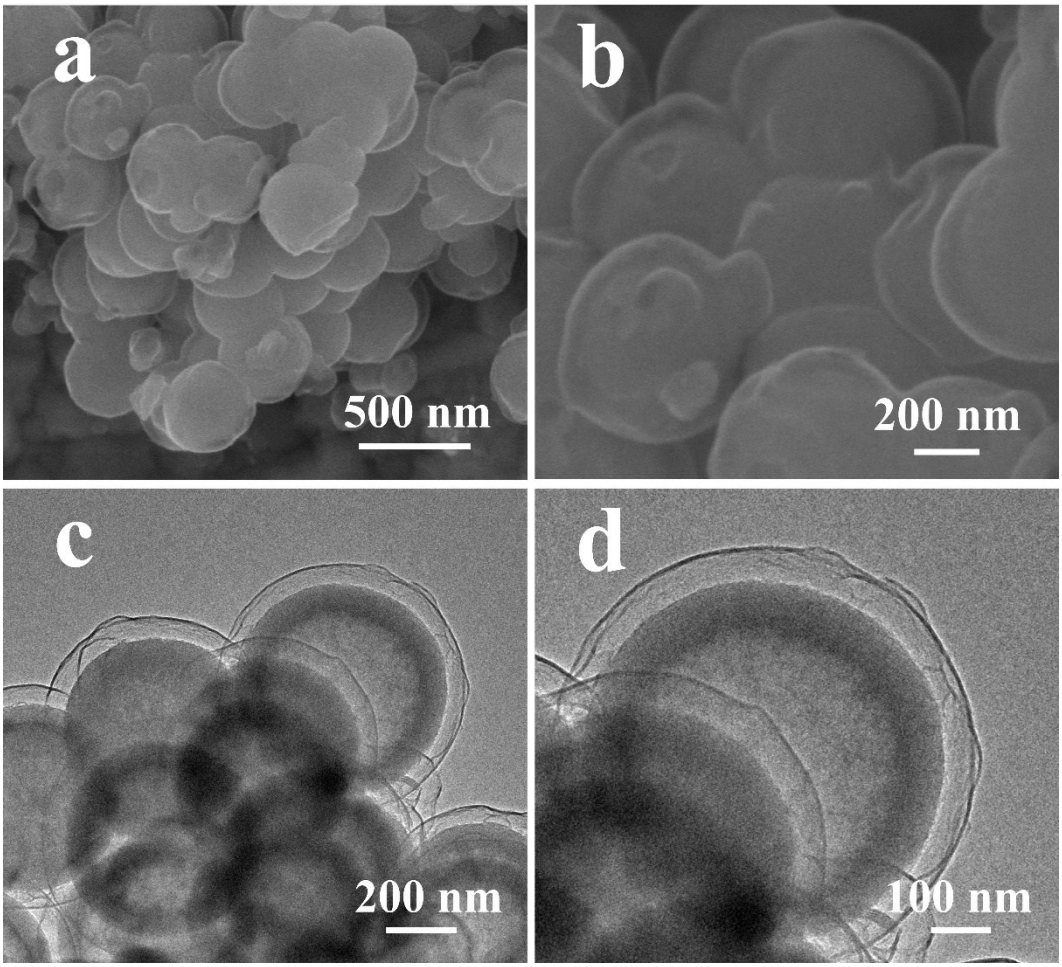

Figure S3. SEM images (a) and (b), and TEM images of (c) and (d) of SiO_2@C ball-in-ball hollow spheres.

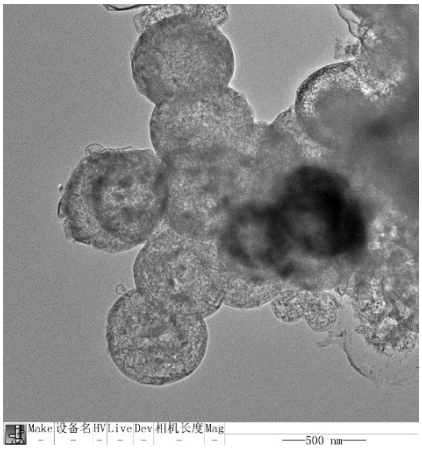

Figure S4. TEM image of Si@SiC@C.

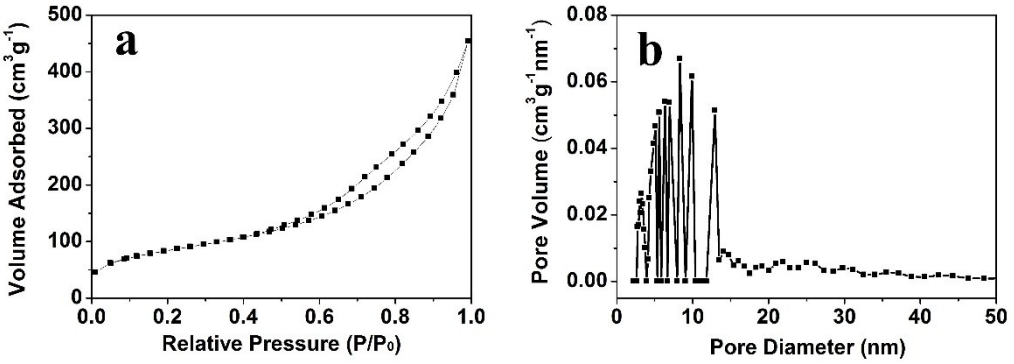

Figure S5. (a) Nitrogen adsorption/desorption isotherms obtained at 77 K and (b) pore size distribution of Si@C ball-in-ball hollow spheres.

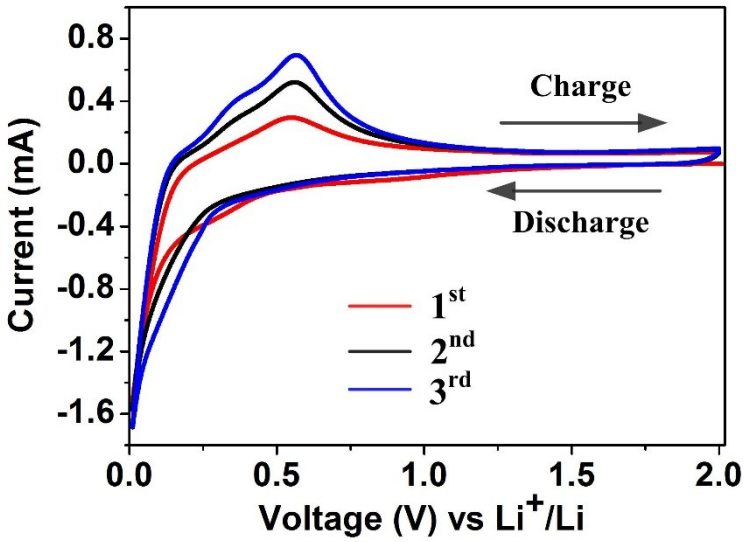

Figure S6. CV curves of Si@C ball-in-ball hollow spheres.

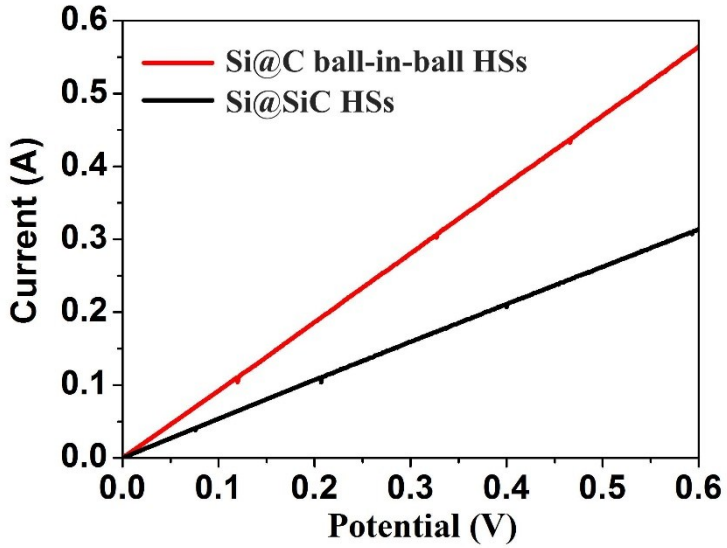

Figure S7. Conductivity of Si@C ball-in-ball hollow spheres and Si@SiC hollow spheres.

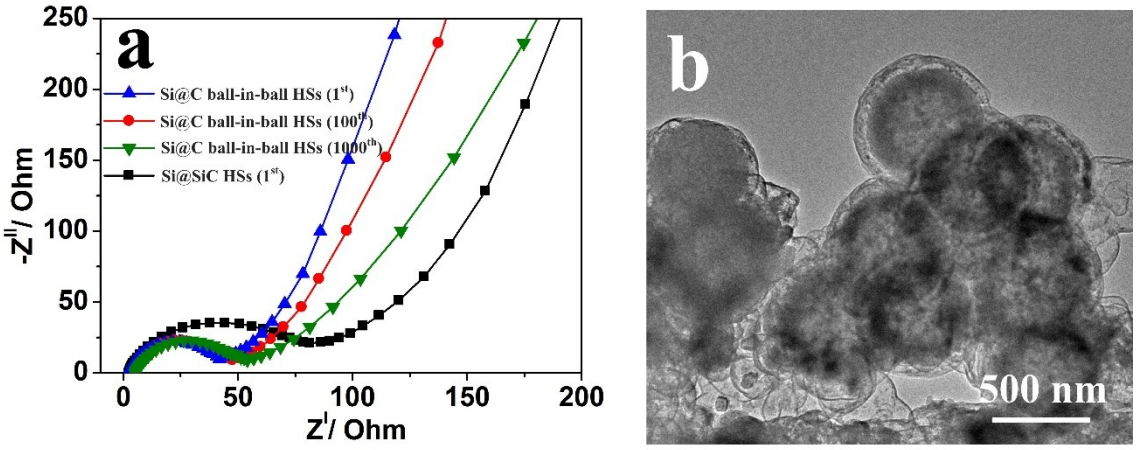

Figure S8. (a) Nyquist plots of Si@C ball-in-ball hollow spheres and Si@SiC@C hollow spheres.

(b) TEM image of Si@C ball-in-ball hollow spheres after 1000 cycles.

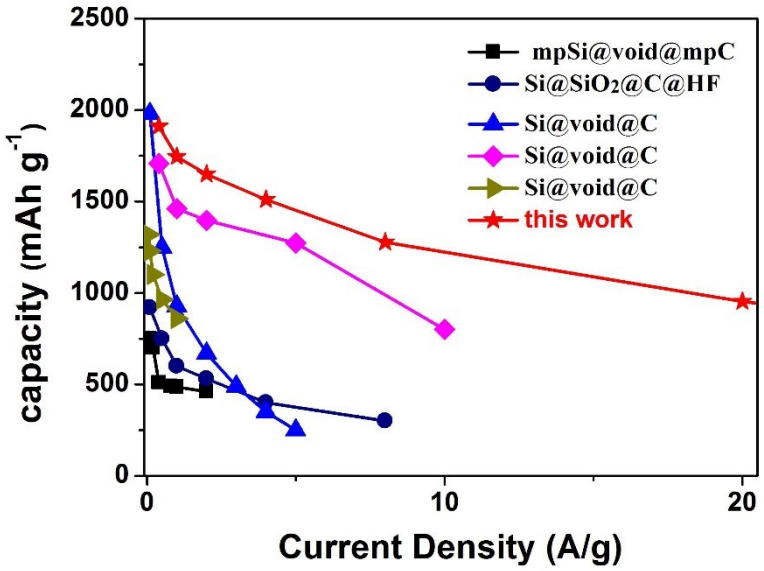

Figure S9. Comparison of capacity at different rates for Si@void@C composite electrode with those of Si/C yolk-shell nanocomposite anodes reported.[1-5]

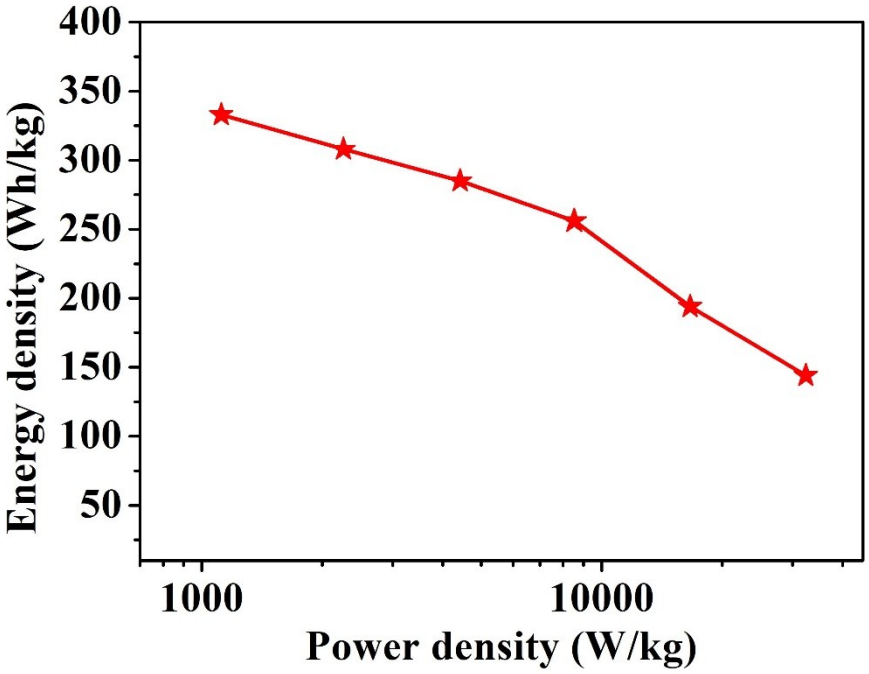

Figure S10. The energy and power density (based on the mass of RAC) of Li || RAC LIC .

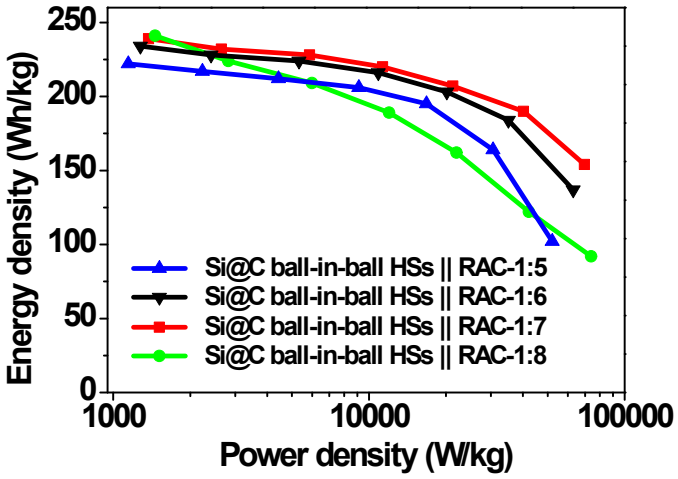

Figure 11. Ragone plot of LICs using Si@C ball-in-ball hollow spheres as anode and RAC as cathode with various mass ratios.

References

[1] L. Pan, H. Wang, D. Gao, S. Chen, L. Tan, L. Li, Chemical Communications 2014, 50, 5878.

[2] L. Su, J. Xie, Y. Xu, L. Wang, Y. Wang, M. Ren, Physical Chemistry Chemical Physics 2015, 17, 17562.

[3] Y. Ru, D. G. Evans, H. Zhu, W. Yang, Rsc Advances 2014, 4, 71.

[4] X. Li, P. Meduri, X. Chen, W. Qi, M. H. Engelhard, W. Xu, F. Ding, J. Xiao, W. Wang, C. Wang, Journal of Materials Chemistry 2012, 22, 11014.

[5] B. Li, R. Qi, J. Zai, F. Du, C. Xue, Y. Jin, C. Jin, Z. Ma, X. Qian, Small 2016, 12, 5281.